

Time Step Rescaling Recovers Continuous-Time Dynamical Properties for Discrete-Time Langevin Integration of Nonequilibrium Systems

David A. Sivak,^{*,†,‡,¶} John D. Chodera,[‡] and Gavin E. Crooks[†]

Physical Biosciences Division, Lawrence Berkeley National Laboratory, Berkeley, California 94720, USA, and Computational Biology Program, Memorial Sloan-Kettering Cancer Center, New York, New York 10065, USA

E-mail: david.sivak@ucsf.edu

Abstract

When simulating molecular systems using deterministic equations of motion (*e.g.*, Newtonian dynamics), such equations are generally numerically integrated according to a well-developed set of algorithms that share commonly agreed-upon desirable properties. However, for stochastic equations of motion (*e.g.*, Langevin dynamics), there is still broad disagreement over which integration algorithms are most appropriate. While multiple desiderata have been proposed throughout the literature, consensus on which criteria are important is absent, and no published integration scheme satisfies all desiderata simultaneously. Additional nontrivial complications stem from simulating systems driven out of equilibrium using existing stochastic integration schemes in conjunction with recently-developed nonequilibrium fluctuation theorems. Here, we examine a family of discrete time integration schemes for Langevin dynamics, assessing how each member satisfies a variety of desiderata that have been enumerated in prior efforts to construct suitable Langevin integrators. We show that the incorporation of a novel time step rescaling in the deterministic updates of position and velocity can correct a number of dynamical defects in these integrators. Finally, we identify a particular

splitting (related to the velocity Verlet discretization) that has essentially universally appropriate properties for the simulation of Langevin dynamics for molecular systems in equilibrium, nonequilibrium, and path sampling contexts.

Keywords: Langevin dynamics, discrete integrators, path action.

Introduction

Simulating the dynamics of molecular systems on a digital computer requires that the equations of motion be discretized. The resulting discrete-time integration algorithm that governs the updates of particle positions and velocities will necessarily have properties that differ from the continuous equations of motion on which it was based. To construct such an algorithm, one must decide which properties of the original dynamics should be preserved. Even then, a multitude of integration schemes may satisfy these properties and still recover the continuous stochastic equations of motion in the limit of an infinitesimally small time step.

For integrating the deterministic classical equations of motion prescribed by Newtonian dynamics, explicit symplectic integration schemes such as velocity Verlet are now widely regarded as being optimal for condensed matter systems for a number of reasons: they are reversible, simple to implement, preserve phase space volume, require minimal force evaluations, and are generally stable over long integration times.^{1–5}

For stochastic equations of motion—in which the influence of some system components (often the solvent) are not represented explicitly, but instead by random

^{*}To whom correspondence should be addressed

[†]Physical Biosciences Division, Lawrence Berkeley National Laboratory, Berkeley, California 94720, USA

[‡]Computational Biology Program, Memorial Sloan-Kettering Cancer Center, New York, New York 10065, USA

[¶]Current address: Center for Systems and Synthetic Biology, University of California, San Francisco, California 94158, USA

collisions with fictitious particles—no such generally-adopted integrator yet exists. In particular, the dynamics produced by existing algorithms differ (in a time step dependent manner) in important respects from the dynamics of the continuous equations of motion. Nevertheless, significant effort has been devoted to developing such stochastic integrators due to their utility in simulating many systems of interest to the chemical, biophysical, and physical sciences.

Driven nonequilibrium systems present their own set of special challenges. For example, a powerful set of nonequilibrium work fluctuation theorems⁶ permit the computation of equilibrium properties of systems from their nonequilibrium statistics, but require as input the distribution of work values associated with the ensemble of trajectories. Calculations that use naive analogies of the work for continuous dynamics—failing to take into account details of the discrete integration scheme—possess systematic biases.⁷

Here, we consider various choices that could be made in constructing discrete-time integration schemes for Langevin dynamics. By examining the various possible Strang splittings of the Langevin Liouville operator, incorporating a novel time step rescaling [Eq. (Eq. (15))], and comparing their resulting properties to several desiderata that have been enumerated in the literature over recent decades, we show how it is possible to simultaneously satisfy nearly all these criteria with a single integration scheme [Eq. (Eq. (7))] that is generally applicable, simple to implement, computationally efficient, and produces thermodynamically-consistent nonequilibrium statistics.

Theory

The Langevin equation

A standard framework for the stochastic simulation of molecular systems assumes that the variables of interest evolve according to Langevin dynamics with uncorrelated Gaussian noise,⁸ which represents interactions with the surrounding environment through frictional drag and stochastic collisions with fictitious bath particles:

$$dr = v dt \quad (1a)$$

$$dv = \frac{f(t)}{m} dt - \gamma v dt + \sqrt{\frac{2\gamma}{\beta m}} dW(t). \quad (1b)$$

Here r and v are time-dependent position and velocity, m is mass, $\beta = 1/k_B T$, k_B is Boltzmann’s constant, T is

the temperature of the environment, γ is a friction coefficient (with dimensions of inverse time), and $W(t)$ is a standard Wiener process. The force $f(t)$ is due to the (in general time-dependent) Hamiltonian $\mathcal{H}(t)$ on the system with position $r(t)$, as determined by the derivative of the potential energy, $-\partial\mathcal{H}(t)/\partial r$, evaluated at $r(t)$. For multi-dimensional, multi-particle systems, r , v , f , and dW are vectors, and m is a diagonal matrix (see Supporting Information, “Multiple dimensions.”)

While these equations of motion can be solved exactly for some simple systems, nearly all complex systems of interest require computational techniques in order to generate dynamical trajectories. On digital computers, this requires discretization of time. The selection of an appropriate discrete time integration scheme is made difficult by the fact that *many* discretizations may exist that recover the same continuous stochastic differential equations of motion in the limit of an infinitesimally small time step, but these schemes may possess very different properties for finite time steps.

Desiderata

Finite time step integrators for molecular systems cannot hope to *exactly* reproduce snapshots from the dynamical trajectories of the continuous equations of motion of a real physical system. Imprecision of experimental measurements ensures that simulated initial conditions necessarily deviate from ‘true’ ones, and Lyapunov instability of even deterministic dynamics ensures the rapid chaotic growth of such deviations, making the exact reproduction of a particular trajectory impossible even were it desirable.³ Moreover, artifacts are inevitably introduced when one discretizes continuous equations of motion in a straightforward manner: dynamical motion increasingly diverges from that of continuous equations of motion with increasing friction and/or time step. Instead, the goal is often to reproduce certain statistical (often observable) properties of the system, especially in terms of correlation functions and (possibly time-dependent) ensemble expectations given a set of initial conditions. Thus, a desirable approximation scheme should share certain statistical and dynamical properties of the ensemble of trajectories associated with the exact equations of motion, in lieu of being able to exactly integrate trajectories.

Pastor, *et al.*⁹ proposed that a useful discrete-time integrator should reproduce seven quantities associated with the continuous-time equations of motion: for a free particle (zero-force), the mean-squared displacement (MSD) as a function of time, the mean-squared velocity (MSV), and the velocity autocorrelation func-

External Force	Quantity	Expression	Continuous-Limit Value
zero	mean-squared displacement	$\langle r^2(n) \rangle$	$\frac{2}{\beta m \gamma} n \Delta t$
	mean-squared velocity	$\langle v^2(n) \rangle$	$\frac{1}{\beta m}$
	velocity autocorrelation	$\langle v(n)v(n+n') \rangle$	$\frac{1}{\beta m} e^{-\gamma n' \Delta t}$
uniform, f	terminal drift	$\frac{\langle r(n+1) - r(n) \rangle}{\Delta t}$	$\frac{f}{m \gamma}$
		$= \frac{\langle r(n+\frac{1}{2}) - r(n-\frac{1}{2}) \rangle}{\Delta t}$	
linear, $-kr$	mean-squared displacement	$\langle r^2(n) \rangle$	$\frac{1}{\beta \bar{k}}$
	mean-squared velocity	$\langle v^2(n) \rangle$	$\frac{1}{\beta m}$
		$m \langle v^2(n) \rangle - k \langle r^2(n) \rangle$	0
		$m \langle v^2(n) \rangle - k \langle r^2(n+\frac{1}{2}) \rangle - k \langle r^2(n+\frac{1}{2}) \rangle$	

Table 1: Definition of dynamical properties. Angled brackets denote an average over the ensemble of phase-space trajectories produced by a given integration scheme. We consider an integration scheme to preserve a given dynamical property as long as the scheme produces the continuous-limit value of that dynamical property at some point during the full time step, even if it produces different values at other points.

tion (VAC); for a uniform external force, the terminal velocity; and for a harmonic potential (linear force), the MSD, MSV, and the virial. In Table Table 1, we define these desired dynamical properties and list their analytically computed values for the continuous equations of motion. In Supporting Information, “Determination of rescaling parameters,” we describe in detail the calculation of these quantities for our family of integrators.

One should not expect a discrete algorithm to give meaningful results on timescales less than a single time step. Those users who prefer to treat a discrete algorithm as a black box will be most interested in integrators that satisfy given dynamical properties at integer time steps. Those willing to look further under the hood would need to know at which specific point within a given time step to measure a given dynamical quantity to recover (or most closely approximate) the continuous-limit value. Thus, we examine dynamical properties at both integer and fractional time steps.

There are several other criteria that one may want an integrator to satisfy, not the least of which being ease of implementation and analysis. Additionally, an integrator that is computationally efficient should have an accuracy that scales reasonably with time step length (here, quadratically, the same accuracy order as popular symplectic integration schemes for deterministic dynamics such as velocity Verlet), permitting relatively large time steps; minimize the number of force evaluations (one per time step) so as to minimize computational effort; and easily incorporate constraints (typically reflecting covalent chemical bonds to light elements such as hydrogen) that push the integrator stability limit to larger time step. Path sampling¹⁰ or path reweighting^{11,12} strategies often require an integrator that induces an irreducible Markov chain (*i.e.*, it is possible to transition from any phase space point to any other in a single time step through specific choice of the random variables¹³) and that for a given trajectory has a readily evaluated path action that governs the probability of that trajectory within the dynamical ensemble.

Indeed, the task is further complicated when the integrator must produce thermodynamically-consistent nonequilibrium simulations. To facilitate the use of nonequilibrium fluctuation relations⁶ and estimators derived from them, the integrator must properly split dynamics into stochastic, explicit Hamiltonian-update, and deterministic substeps that distinguish between the heat, work, and shadow work.¹⁴ For the calculated works to be thermodynamically meaningful, the integrator must also have a form symmetric under time-reversal.

Pastor, *et al.* demonstrate that no member of their

family of overdamped integrators can simultaneously satisfy more than four of their seven desired dynamical properties. Many other underdamped discretizations of the Langevin equation have been proposed^{15–25} that achieve some subset of these enumerated desiderata, yet there still is no widespread agreement on an integrator that performs satisfactorily for a broad set of purposes.

Resolution: time step rescaling

Drawing inspiration from several popular integrators, in this paper we derive a simple family of integrators that split the different update types to permit the definition of thermodynamically meaningful quantities for work and heat. With a novel rescaling of the time step, the resulting dynamics preserves five of Pastor *et al.*’s seven dynamical properties for any values of friction and time step (six if fractional time step values are also considered), and furthermore satisfies all of the other desiderata enumerated above, including its utility for nonequilibrium simulations and schemes involving path sampling or reweighting. The resulting integrator represents a stochastic generalization of velocity Verlet, is simple to implement, and could be a general all-purpose replacement for the various discrete-time Langevin integrators now in use.

In sampling contexts, this time step rescaling does slow the exploration of conformational space if the raw integration time step Δt is not concomitantly increased. We believe that such a time step rescaling permits a larger raw time step, but exactly how much larger Δt can be increased (and hence to what extent sampling efficiency can be recovered or even improved) before reaching the stability limit (or some other integration pathology) remains an open question. Addressing this potentially system-specific issue requires further theoretical and numerical investigation, which is beyond the scope of this paper.

Integrator Splitting

We derive a family of integrators by splitting the time evolution operator into stochastic and deterministic components²⁰ and choosing the adjustable parameters to match dynamical quantities from the continuous equations of motion. We write the one-dimensional version here, but the generalization to multiple dimensions is straightforward (see the Supporting Information, “Multiple dimensions”). The Langevin Liouville operator (sometimes termed the *Liouvillian*)²⁶ can be

naturally written as a sum of four parts $\mathcal{L} = \mathcal{L}_o + \mathcal{L}_v + \mathcal{L}_r + \mathcal{L}_h$. The first operator represents stochastic thermalization²⁷ via an Ornstein-Uhlenbeck operator,

$$\mathcal{L}_o = -\gamma \frac{\partial}{\partial v} v - \frac{\gamma}{\beta m} \frac{\partial^2}{\partial v^2}; \quad (2)$$

the next two operators represent deterministic Newtonian evolution of velocity and position,

$$\mathcal{L}_v = \frac{f}{m} \frac{\partial}{\partial v}, \quad \mathcal{L}_r = v \frac{\partial}{\partial r}; \quad (3)$$

and the last operator represents the time evolution of the system Hamiltonian according to the predetermined schedule (or *protocol*) Λ ,

$$e^{\Delta t \mathcal{L}_h} \mathcal{H}(n) = \mathcal{H}(n+1), \quad (4)$$

where n denotes the time step index and $t = n\Delta t$ the simulation clock time for time step Δt . (Note that in the case of a time-independent Hamiltonian, $e^{\Delta t \mathcal{L}_h}$ is the identity operator.) Similar to several other integrators,^{17,20,21,28,29} we approximate the dynamics over a time Δt by applying a series of Strang (symmetric Trotter) operator splittings,³⁰

$$e^{\Delta t [A+B+C+D]} \quad (5a)$$

$$= e^{\frac{\Delta t}{2} A} e^{\Delta t [B+C+D]} e^{\frac{\Delta t}{2} A} + \mathcal{O}(\Delta t^3) \quad (5b)$$

$$= e^{\frac{\Delta t}{2} A} e^{\frac{\Delta t}{2} B} e^{\Delta t [C+D]} e^{\frac{\Delta t}{2} B} e^{\frac{\Delta t}{2} A} + \mathcal{O}(\Delta t^3) \quad (5c)$$

$$= e^{\frac{\Delta t}{2} A} e^{\frac{\Delta t}{2} B} e^{\frac{\Delta t}{2} C} e^{\Delta t D} e^{\frac{\Delta t}{2} C} e^{\frac{\Delta t}{2} B} e^{\frac{\Delta t}{2} A} + \mathcal{O}(\Delta t^3), \quad (5d)$$

where (A, B, C, D) represents a permutation of $(\mathcal{L}_o, \mathcal{L}_v, \mathcal{L}_r, \mathcal{L}_h)$.

There are six Strang splittings of the Liouville operators $\mathcal{L}_o, \mathcal{L}_r, \mathcal{L}_v$. The Hamiltonian update operator \mathcal{L}_h commutes with \mathcal{L}_o and with \mathcal{L}_r , so for each of these six splittings there are only two unique placements of \mathcal{L}_h . For each of the six splittings, one placement of \mathcal{L}_h interleaves the position, Hamiltonian, and deterministic velocity updates in such a way as to require multiple force evaluations per step, making the scheme computationally inefficient. Thus there are six distinct splittings that each give rise to different finite time step dynamics and require only one force evaluation per step. Notably, because the error in each Strang splitting is $\mathcal{O}(\Delta t^3)$, all are identical to the true Liouville operator \mathcal{L} in the limit $\Delta t \rightarrow 0^+$.

One such splitting is a stochastic generalization of Velocity Verlet that we call OVRVO (to denote the respective ordering of Ornstein-Uhlenbeck (O), deterministic velocity (V), and deterministic position (R) up-

dates (in analogy to the nomenclature of Leimkuhler and Matthews²⁵),

$$e^{\Delta t [\mathcal{L}_o + \mathcal{L}_v + \mathcal{L}_r + \mathcal{L}_h]} \simeq \underbrace{e^{\frac{\Delta t}{2} \mathcal{L}_o}}_a \underbrace{e^{\frac{\Delta t}{2} \mathcal{L}_v}}_b \underbrace{e^{\frac{\Delta t}{2} \mathcal{L}_r}}_c \underbrace{e^{\Delta t \mathcal{L}_h}}_d \underbrace{e^{\frac{\Delta t}{2} \mathcal{L}_r}}_e \underbrace{e^{\frac{\Delta t}{2} \mathcal{L}_v}}_f \underbrace{e^{\frac{\Delta t}{2} \mathcal{L}_o}}_g. \quad (6)$$

The Hamiltonian-update step is placed to minimize the number of force evaluations per time step.

For this operator splitting, a single update step that advances the simulation clock by Δt is given explicitly by:

$$v(n + \frac{1}{4}) = \sqrt{a} v(n) + \sqrt{\frac{1-a}{\beta m}} \mathcal{N}^+(n) \quad (7a)$$

$$v(n + \frac{1}{2}) = v(n + \frac{1}{4}) + \frac{b \Delta t}{2} \frac{f(n)}{m} \quad (7b)$$

$$r(n + \frac{1}{2}) = r(n) + \frac{b \Delta t}{2} v(n + \frac{1}{2}) \quad (7c)$$

$$\mathcal{H}(n) \rightarrow \mathcal{H}(n+1) \quad (7d)$$

$$r(n+1) = r(n + \frac{1}{2}) + \frac{b \Delta t}{2} v(n + \frac{1}{2}) \quad (7e)$$

$$v(n + \frac{3}{4}) = v(n + \frac{1}{2}) + \frac{b \Delta t}{2} \frac{f(n+1)}{m} \quad (7f)$$

$$v(n+1) = \sqrt{a} v(n + \frac{3}{4}) + \sqrt{\frac{1-a}{\beta m}} \mathcal{N}^-(n+1). \quad (7g)$$

Here, $a = \exp(-\gamma \Delta t)$, and \mathcal{N}^+ and \mathcal{N}^- are independent, normally distributed random variables with zero mean and unit variance (hence, when scaled by $(\beta m)^{-1/2}$, distributed according to the equilibrium Maxwell-Boltzmann velocity distribution).

The substeps in Eq. (Eq. (7)) are the finite difference expressions of the corresponding suboperators in Eq. (Eq. (6)). The initial (a) and final (g) operators randomize the velocity and leave the position unchanged, mixing the old velocity with a Maxwell-Boltzmann random variate (with old velocity weighted according to $a = \exp[-\gamma \Delta t]$). These operators can be analytically integrated to give the first (Eq. (7a)) and last (Eq. (7g)) substeps that are stochastic, Markovian, and detailed-balanced (with respect to the true canonical measure³¹).^{20,32} The operators (b) and (f) correspond to deterministic velocity updates, while (c) and (e) correspond to deterministic position updates. Together they are approximated by the finite difference expressions of substeps [Eq. (7b), Eq. (7c), Eq. (7e), Eq. (7f)], which together constitute the deterministic and symplectic velocity Verlet integrator,^{1,28} but slightly altered by an effective time step rescaling $0 \leq b \leq 1$, chosen to maintain the continuous-limit zero-force diffu-

sion coefficient and terminal drift under a uniform external force, regardless of friction coefficient or time step (derived in Supporting Information, “Determination of rescaling parameters”). In the limit $\Delta t \rightarrow 0$ this rescaling factor b converges to unity and the splitting converges to the continuous-time equation of motion [Eq. (Eq. (1))]. Operator (d) and its finite difference expression as Eq. (Eq. (7d)) makes explicit the midpoint Hamiltonian update. Note that several other popular integrators do not explicitly include the update of the system Hamiltonian, presumably because they are not concerned with calculating distributions of the work generated by explicit Hamiltonian changes.

The alternative splittings with one force evaluation per time step include ORVRO (a stochastic generalization of position Verlet²⁸),

$$e^{\Delta t[\mathcal{L}_o + \mathcal{L}_v + \mathcal{L}_r + \mathcal{L}_h]} \simeq e^{\frac{\Delta t}{2}\mathcal{L}_o} e^{\frac{\Delta t}{2}\mathcal{L}_r} e^{\frac{\Delta t}{2}\mathcal{L}_h} e^{\Delta t\mathcal{L}_v} e^{\frac{\Delta t}{2}\mathcal{L}_h} e^{\frac{\Delta t}{2}\mathcal{L}_r} e^{\frac{\Delta t}{2}\mathcal{L}_o}; \quad (8)$$

RVOVR (an explicit Hamiltonian-update generalization of Leimkuhler and Matthew’s ‘ABOBA’),

$$e^{\Delta t[\mathcal{L}_o + \mathcal{L}_v + \mathcal{L}_r + \mathcal{L}_h]} \simeq e^{\frac{\Delta t}{2}\mathcal{L}_r} e^{\frac{\Delta t}{2}\mathcal{L}_h} e^{\frac{\Delta t}{2}\mathcal{L}_v} e^{\Delta t\mathcal{L}_o} e^{\frac{\Delta t}{2}\mathcal{L}_v} e^{\frac{\Delta t}{2}\mathcal{L}_h} e^{\frac{\Delta t}{2}\mathcal{L}_r}, \quad (9)$$

VRORV (an explicit Hamiltonian-update generalization of Leimkuhler and Matthew’s ‘BAOAB’),

$$e^{\Delta t[\mathcal{L}_o + \mathcal{L}_v + \mathcal{L}_r + \mathcal{L}_h]} \simeq e^{\frac{\Delta t}{2}\mathcal{L}_v} e^{\frac{\Delta t}{2}\mathcal{L}_r} e^{\frac{\Delta t}{2}\mathcal{L}_h} e^{\Delta t\mathcal{L}_o} e^{\frac{\Delta t}{2}\mathcal{L}_h} e^{\frac{\Delta t}{2}\mathcal{L}_r} e^{\frac{\Delta t}{2}\mathcal{L}_v}; \quad (10)$$

ROVOR,

$$e^{\Delta t[\mathcal{L}_o + \mathcal{L}_v + \mathcal{L}_r + \mathcal{L}_h]} \simeq e^{\frac{\Delta t}{2}\mathcal{L}_r} e^{\frac{\Delta t}{2}\mathcal{L}_o} e^{\frac{\Delta t}{2}\mathcal{L}_h} e^{\Delta t\mathcal{L}_v} e^{\frac{\Delta t}{2}\mathcal{L}_h} e^{\frac{\Delta t}{2}\mathcal{L}_o} e^{\frac{\Delta t}{2}\mathcal{L}_r}, \quad (11)$$

and VOROV,

$$e^{\Delta t[\mathcal{L}_o + \mathcal{L}_v + \mathcal{L}_r + \mathcal{L}_h]} \simeq e^{\frac{\Delta t}{2}\mathcal{L}_v} e^{\frac{\Delta t}{2}\mathcal{L}_o} e^{\frac{\Delta t}{2}\mathcal{L}_r} e^{\Delta t\mathcal{L}_h} e^{\frac{\Delta t}{2}\mathcal{L}_r} e^{\frac{\Delta t}{2}\mathcal{L}_o} e^{\frac{\Delta t}{2}\mathcal{L}_v}. \quad (12)$$

Since for a single time step Δt the error is $O(\Delta t^3)$ for any of these Strang splittings, when applied over $N = t/\Delta t$ time steps the global error is $O(\Delta t^2)$. Fig. Figure 1 confirms that OVRVO errors in the energy are second order in the time step Δt .

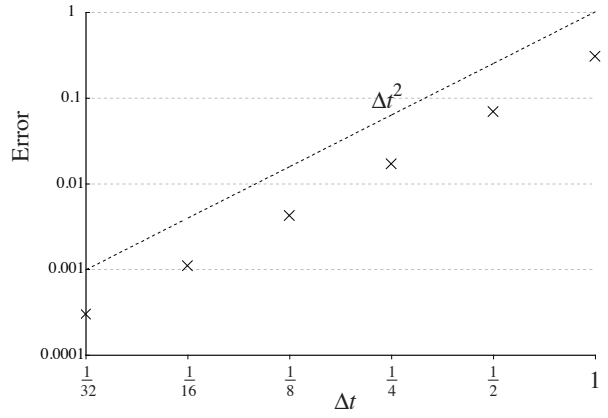


Figure 1: **Numerical demonstration that the errors in energy of the OVRVO integrator [Eq. (Eq. (7))]** are second order in Δt . Here, we use a previously described model system¹⁹ of a harmonic potential, with unit spring constant, friction coefficient, temperature, and mass, with initial conditions $r(0) = v(0) = 0$. The error is the absolute deviation of the estimate of $\langle r^2(1) + v^2(1) \rangle = 0.9796111900\dots$ (twice the energy) computed by ensemble averaging over 10^8 independent realizations. Standard errors of the mean are substantially smaller than the symbol size. The line is the graph of the function Δt^2 .

Time step rescaling recovers dynamical properties

Standard integrators implicitly set the parameter b to unity in Eq. (7b), Eq. (7c), Eq. (7e), Eq. (7f). However, we show later that a non-unit b recovers, for arbitrarily-large time step, the continuous-limit values of important dynamical quantities. The time step rescaling can be most simply derived by noting that in the absence of a potential, for any of the six splittings, a trajectory is isomorphic to a semi-flexible Gaussian polymer chain:³³ the set of positions correspond to the beads on the polymer chain, and the displacement vectors during single time steps correspond to the inter-monomer bond vectors in the chain. In one dimension, the displacement is a normally distributed random variable with zero mean and variance $\sigma_0^2 = (b\Delta t)^2/(\beta m)$ (in accordance with Maxwell-Boltzmann velocity statistics and the time interval $b\Delta t$), and the autocorrelation between velocities separated by N steps decays exponentially as

$$\langle v(N) v(0) \rangle = \frac{a^N}{\beta m}. \quad (13)$$

For this system the mean square displacement in the large time ($\gamma t \gg 1$) limit is³³

$$\langle [r(N) - r(0)]^2 \rangle = N \sigma_0^2 \frac{1+a}{1-a} \quad (14a)$$

$$= N \frac{(b\Delta t)^2}{\beta m} \coth \frac{\gamma \Delta t}{2}. \quad (14b)$$

The time step rescaling b results from equating this expression to the mean-squared displacement of a freely diffusing particle in one dimension, $2Dt = 2t/(\beta m \gamma)$, for a total simulation time over N steps, $t = N \Delta t$. In particular, the time step used in the position update step is rescaled by the factor

$$b = \sqrt{\frac{2}{\gamma \Delta t} \tanh \frac{\gamma \Delta t}{2}}, \quad (15)$$

ensuring that the effective free-particle diffusion constant is independent of time step length (see Fig. Figure 2). In the low friction limit $\gamma \Delta t \ll 1$, $b = 1 - O([\gamma \Delta t]^2)$, and in the high friction limit $\gamma \Delta t \gg 1$, $b = \sqrt{2/(\gamma \Delta t)}$.

Note that even though the position update utilizes an effective time step of $b\Delta t$, the simulation clock is still advanced by the full time step Δt . The zero-force MSV and VAC and the uniform-force terminal drift are unaffected by the choice of b . We derive the time step rescaling from a different perspective and in more detail in Supporting Information, “Determination of rescaling parameters.”

Integrator properties

OVRVO generalizes other popular integrators

For an explicitly time-independent system Hamiltonian, this family of integrators reduces to various other schemes in certain limits or approximations. At zero friction, $\gamma = 0$ and $a = b = 1$, thus stochastic substeps have no effect, so OVRVO, VRORV, and VOROV are identical to the deterministic velocity Verlet integrator, whereas ORVRO, RVOVR, and ROVOR are identical to position Verlet. In the high-friction or long-time limit, $a = 0$ and $b = \sqrt{2/(\gamma \Delta t)}$, and OVRVO reduces to the Euler integrator for overdamped Langevin dynamics³⁴ (also known as the Euler-Maruyama method³⁵),

$$r(n+1) = r(n) + \frac{\Delta t}{\gamma} \frac{f(n)}{m} + \sqrt{\frac{2\Delta t}{\beta m \gamma}} \mathcal{N}(n). \quad (16)$$

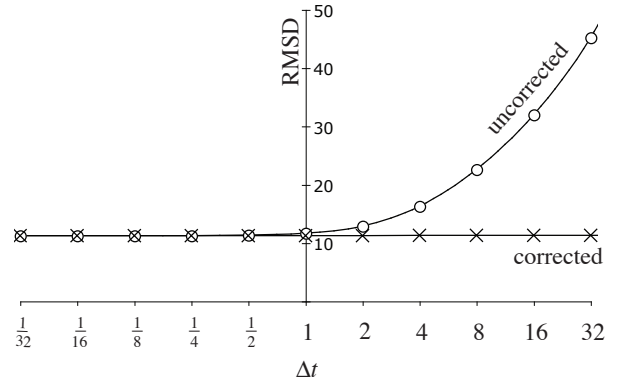


Figure 2: Time step rescaling recovers correct field-free diffusion as a function of time step.

Root mean-squared displacement versus relative time step length Δt at time $t = 64$ for a freely diffusing particle in one dimension, with unit mass, temperature, and friction coefficient, subject to the OVRVO integrator [Eq. (Eq. (7))] without time step rescaling, $b = 1$ (\circ), or with time step rescaling, Eq. (Eq. (15)) (\times).

ROVOR and VOROV interpose a velocity randomization substep between the deterministic velocity and position updates. In this $\gamma \Delta t \gg 1$ limit, the velocity is completely randomized before each position-update substep, and thus the position updates are completely independent of the Hamiltonian. The other four splittings preserve the influence of the Hamiltonian on the dynamics even in this limit of large friction (or large time step).

OVRVO also reduces to several other popular integrators in other limits or approximations. If the effective time step rescaling for the deterministic substeps is omitted, such that $b = 1$, then OVRVO is equivalent to an integrator described by Adjanor, Athènes, and Calvo;¹⁸ and by Bussi and Parrinello.²⁰ If we also combine all stochastic and deterministic velocity updates [Eq. (7f), Eq. (7g), Eq. (7a), Eq. (7b)], we recover the integrator of Athènes;¹⁶ and recasting the Athènes integrator as a Verlet-style integrator (only monitoring position) we converge with the Brünger-Brooks-Karplus (BBK) integrator¹⁵ in the low friction limit. If instead we only combine adjacent pairs of stochastic and deterministic velocity updates [(Eq. (7a)) with (Eq. (7b)), (Eq. (7f)) with (Eq. (7g))] (still with no time step rescaling) we produce the low friction limit of the Langevin Leapfrog integrator of Izaguirre, Sweet, and Pande.^{11,22}

Nonequilibrium work

There is significant interest in probing the probability distribution of work required during a nonequilibrium driving process, which via the work fluctuation theorems⁶ can report on various system properties. Such usage requires careful splitting of thermodynamically distinct energy changes.⁷

The total energy change ΔE during the n th full time step of OVRVO can be cleanly separated into heat Q , protocol work W_{prot} , and shadow work W_{shad} :⁷

$$\Delta E = Q + W \quad (17a)$$

$$= Q + W_{\text{prot}} + W_{\text{shad}} \quad (17b)$$

$$Q = \mathcal{T}(v(n + \frac{1}{4})) - \mathcal{T}(v(n)) \quad (17c)$$

$$+ \mathcal{T}(v(n + 1)) - \mathcal{T}(v(n + \frac{3}{4}))$$

$$W_{\text{prot}} = \mathcal{U}(r(n + \frac{1}{2}), n + 1) - \mathcal{U}(r(n + \frac{1}{2}), n) \quad (17d)$$

$$W_{\text{shad}} = \mathcal{T}(v(n + \frac{1}{2})) - \mathcal{T}(v(n + \frac{1}{4})) \quad (17e)$$

$$+ \mathcal{U}(r(n + \frac{1}{2}), n) - \mathcal{U}(r(n), n)$$

$$+ \mathcal{U}(r(n + 1), n + 1) - \mathcal{U}(r(n + \frac{1}{2}), n + 1)$$

$$+ \mathcal{T}(v(n + \frac{3}{4})) - \mathcal{T}(v(n + \frac{1}{2})).$$

Here, $\mathcal{U}(r, n)$ is the potential energy for configuration r under Hamiltonian $\mathcal{H}(n)$, and $\mathcal{T}(v) = \frac{1}{2}mv^2$ is the kinetic energy for velocity v . The five other splittings permit similar decompositions of energy changes into heat, protocol work, and shadow work.

Constraints

Constraints, such as rigid bond lengths, can be readily incorporated into the dynamics using standard techniques.²⁴ The symplectic part of the integrator can be constrained with the standard RATTLE [Eq. (7b), Eq. (7f)] algorithm.^{3,36} Since RATTLE is symplectic if iterated to convergence,³⁷ adding constraints does not interfere with the underlying reversibility of the dynamics. Similarly, the velocity randomization substeps, Eqs. (Eq. (7a)) and (Eq. (7g)), can be constrained with RATTLE, which modifies the heat flow, but preserves detailed balance.²⁴ Consequently, constrained versions of this family of integrators still obeys the precepts of nonequilibrium thermodynamics,⁷ with the same definitions of heat, protocol work, and shadow work [Eq. (Eq. (17))], provided that the definition of free energy is altered to account for the constrained degrees of freedom.²⁴

Computational efficiency

All six splittings require one force evaluation per time step. For OVRVO, for example, the force in substep (Eq. (7f)) is identical to the force in substep (Eq. (7b)) of the next time interval. Measuring heat requires two evaluations of kinetic energy per time step for all six splittings, for OVRVO just after substep (Eq. (7a)) and just before substep (Eq. (7g)). Separately measuring protocol work and shadow work requires two potential energy evaluations per time step, once each just before and after the Hamiltonian-update substep. Shadow work measurement also requires the kinetic energy evaluations already needed to measure heat, as shadow work and heat are the only processes that change the kinetic energy.

However, if only the total thermodynamic work $W = \Delta E - Q$ is of interest, this can be calculated given the heat $Q^{(n)}$ during each step $n \rightarrow n + 1$ [easily accumulated during integration using Eq. (Eq. (17c))] and the total energy at the beginning and end of the simulation,

$$W = \mathcal{U}(r(N), N) + \mathcal{T}(v(N)) - \mathcal{U}(r(0), 0) - \mathcal{T}(v(0))$$

$$- \sum_{n=0}^{N-1} Q^{(n)}. \quad (18)$$

The OVRVO integrator requires two normal random numbers per velocity per time step, one each for the initial [Eq. (Eq. (7a))] and final [Eq. (Eq. (7g))] velocity randomizations. Splitting the velocity randomization across time steps ensures that the dynamics is microscopically reversible and Markovian, and that the induced Markov chain is irreducible. (The two separate randomization steps permit the independent adjustment of the velocity and the position to arbitrary values.¹³) ORVRO and VOROV also induce irreducible Markov chains. RVOVR, VRORV, and ROVOR, by contrast, do not generate irreducible Markov chains: they effectively agglomerate the two velocity randomizations into a single randomization involving one random number, so for a particular new velocity only one position is possible. Irreducibility has utility for path sampling^{10,38–40} and path reweighting^{11,12} schemes, since any proposed discrete time trajectory through phase space is a valid trajectory of an irreducible Markov chain. However, many practical applications do not require strict irreducibility, so one can halve the number of required random variables for OVRVO and ORVRO by combining the last stochastic substep of one full step with the first stochastic substep of the next full step, and for RVOVR and VRORV by combining the two stochastic substeps of a given full step. ROVOR and VOROV

separate their stochastic substeps such that they cannot be easily combined. Leimkuhler and Matthews show that in the high friction limit and at medium time step VRORV with this single velocity randomization (and time-independent Hamiltonian) is second-order accurate when other integrators become first-order.²⁵

When only the total thermodynamic work is of interest, we can combine the last two velocity updates of Eq. (Eq. (7)) with the first two updates from the next step, and combine the two position updates, to give a three substep stochastic Leapfrog integrator:

$$v(n + \frac{1}{2}) = av(n - \frac{1}{2}) + \sqrt{\frac{1-a^2}{\beta m}} \mathcal{N}(n) \quad (19a)$$

$$+ (1+a) \frac{b\Delta t}{2} \frac{f(n)}{m}$$

$$r(n+1) = r(n) + b\Delta t v(n + \frac{1}{2}) \quad (19b)$$

$$\mathcal{H}(n) \rightarrow \mathcal{H}(n+1). \quad (19c)$$

Under these circumstances, RVOVR, ROVOR, and VOROV reduce to similar three substep integrators, but, due to their sequencing of substeps, ORVRO and VRORV each only reduce to a five substep integrator.

Path action

The path action $\mathcal{S}[X]$ is a necessary quantity for many path sampling^{10,38–40} and path reweighting^{11,12} techniques. The conditional path probability functional is a product of single time step probabilities,

$$P[X|x(0), \Lambda] = e^{-\mathcal{S}[X|x(0), \Lambda]} \quad (20a)$$

$$= \prod_{n=0}^{N-1} P[x(n+1)|x(n)]. \quad (20b)$$

Here, X is a trajectory through phase space between $x(0) \equiv \{r(0), v(0)\}$ at time 0 and $x(N\Delta t)$ at $N\Delta t$. Each time step probability is determined by the probability of the requisite random variables, which for ORVRO is

$$P[x(n+1)|x(n)] \quad (21)$$

$$= \frac{\beta m}{b\Delta t(1-a)} p(\mathcal{N}^+(n)) p(\mathcal{N}^-(n+1)).$$

The first factor $\beta m/[b\Delta t(1-a)]$ is the Jacobian for the change of variables from $\{r(n+1), v(n+1)\}$ to $\{\mathcal{N}^+(n), \mathcal{N}^-(n+1)\}$, and the probabilities are normal with zero mean and unit variance,

$$p(\mathcal{N}^\pm) = \frac{1}{\sqrt{2\pi}} \exp\left[-\frac{1}{2}(\mathcal{N}^\pm)^2\right], \quad (22)$$

where

$$\mathcal{N}^+(n) = \sqrt{\frac{\beta m}{1-a}} [v(n + \frac{1}{4}) - \sqrt{a} v(n)] \quad (23a)$$

$$\mathcal{N}^-(n+1) = \sqrt{\frac{\beta m}{1-a}} [v(n+1) - \sqrt{a} v(n + \frac{3}{4})]. \quad (23b)$$

The intermediate velocities can be determined by the initial and final positions and forces,

$$v(n + \frac{1}{4}) = \frac{1}{b\Delta t} [r(n+1) - r(n)] - \frac{b\Delta t}{2} \frac{f(n)}{m} \quad (24a)$$

$$v(n + \frac{3}{4}) = \frac{1}{b\Delta t} [r(n+1) - r(n)] + \frac{b\Delta t}{2} \frac{f(n+1)}{m}. \quad (24b)$$

Combining Eqs. (Eq. (20)-Eq. (24)) gives the action as a function of position and velocity at the unit time steps,

$$\mathcal{S}[X|x(0), \Lambda] = \ln \left[\frac{2\pi(1-a)b\Delta t}{\beta m} \right]^N \quad (25)$$

$$+ \sum_{n=0}^{N-1} \frac{\beta m}{2(1-a)} \left\{ \left(\frac{r(n+1) - r(n)}{b\Delta t} - \frac{b\Delta t}{2} \frac{f(n)}{m} - \sqrt{a} v(n) \right)^2 \right.$$

$$\left. + \left(\sqrt{a} \left[\frac{r(n+1) - r(n)}{b\Delta t} + \frac{b\Delta t}{2} \frac{f(n+1)}{m} \right] - v(n+1) \right)^2 \right\}.$$

The path probability obeys the expected symmetry under time-reversal,⁷ where the work is defined as in [Eq. (17d), Eq. (17e)].

VOROV has a similarly simple expression for the path action. The path action for ORVRO additionally requires the evaluation of the force and its derivative at the half-step position, $r(n + \frac{1}{2})$, hence requires paths of twice as many points, and therefore is of lesser utility. RVOVR, VRORV, and ROVOR induce *reducible* Markov chains and thus these splittings have infinite path actions for the vast preponderance of paths.

Results

All of our Strang splittings lead to seven-substep integration schemes that are time-symmetric; are second-order accurate in Δt ; make Hamiltonian changes explicit; distinguish between heat, protocol work, and shadow work; and easily incorporate constraints. Six of the twelve unique splittings require a single force evaluation per time step and thus are computationally efficient. Setting $a \equiv e^{-\gamma\Delta t}$ and $b \equiv \sqrt{\frac{2}{\gamma\Delta t} \tanh \frac{\gamma\Delta t}{2}}$ gives for all six one-force-evaluation splittings the continuous-limit MSD, MSV, and VAC in the zero-force case, and

the linear-force virial with asymptotic error $O(\Delta t^2)$. The six splittings differ in the remaining desiderata. We summarize their properties in Table Table 2.

Conclusions

As a stochastic generalization of a standard deterministic technique, OVRVO implements what can be considered a form of velocity Verlet with velocity randomization (VVVR). It is an integrator of general utility, satisfying five of Pastor *et al.*'s seven dynamical properties (six if fractional time step quantities are considered), as well as the remaining enumerated desiderata. It is well-suited for the study of nonequilibrium thermodynamics: work is easily measured because the Hamiltonian changes are made explicit, and these measured works are thermodynamically meaningful because OVRVO distinguishes between heat, protocol work, and shadow work. OVRVO's simple form for the path action facilitates its use in trajectory reweighting or path sampling methods. Our novel time step rescaling maintains (for an arbitrary time step) various continuous-limit dynamical quantities, in particular the uniform-force terminal drift and linear-force fluctuations in position and velocity. Further research is required to determine to what extent this rescaling permits a larger raw integration time step, and hence how it affects sampling efficiency. Finally, OVRVO generalizes several popular integration schemes and thus relates naturally to the existing literature. Its extension to a multiple time step integrator⁴¹ is straightforward, requiring only replacement of the inner symplectic step [Eq. (7b)–Eq. (7f)] with a corresponding symplectic multiple time step integrator for deterministic dynamics.

By contrast, alternative splittings suffer from shortcomings of varying severity and number. ROVOR and VOROV produce uniform-force terminal drift and linear-force fluctuations of position and velocity that differ from continuous-limit values, lose Hamiltonian dependence in the limit of large $\gamma\Delta t$, and require two random numbers per time step even for reducible Markov chains. RVOVR and VRORV induce Markov chains that are not irreducible and thus these splittings have limited utility for path-sampling schemes. ORVRO seems similarly useful to OVRVO, but in path sampling applications requires paths with twice the number of points as OVRVO.

Acknowledgement

The authors thank Manuel Athènes (Commissariat à l'Énergie Atomique/Saclay), Gabriel Stoltz (CER-MICS, Ecole des Ponts ParisTech), Benoît Roux (Univ. of Chicago), Jerome P. Nilmeier (Lawrence Livermore Natl. Lab.), Todd Gingrich (UC Berkeley), Jesús A. Izaguirre (Univ. of Notre Dame), Huafeng Xu and Cristian Predescu (D. E. Shaw Research), Patrick Varilly (Univ. of Cambridge), and Michael Shirts (Univ. of Virginia) for enlightening discussions and constructive feedback on the manuscript. J. D. C. acknowledges support from a Distinguished Postdoctoral Fellowship from the California Institute for Quantitative Biosciences (QB3) at the University of California, Berkeley. D. A. S. and G. E. C. were funded by the Office of Basic Energy Sciences of the U.S. Department of Energy under Contract No. DE-AC02-05CH11231. D. A. S. was partially supported by NIGMS Systems Biology Center grant P50 GM081879.

Dedication

The authors dedicate this work to William C. Swope on the occasion of his 60th birthday and celebration of his seminal contributions to the field of molecular simulation. Additionally, JDC would like to acknowledge the mentorship and insightful advice he has provided over many happy years of collaboration.

Supporting Information

Determination of rescaling parameters

Here we determine the coefficients a and b in the OVRVO equations [Eq. 7] by requiring the exact satisfaction of six of the seven dynamical quantities proposed by Pastor, *et al.*⁹ (the linear-force virial is not preserved). Except where noted, the same analysis produces equivalent results for the ORVRO, RVOVR, VRORV, VOROV and ROVOR splittings.

Zero-force mean-squared velocity

The continuous-limit MSV is fixed by the scale of the random velocity fluctuations. In the zero-force case,

Desideratum	OVRVO	ORVRO	RVOVR	VRORV	VOROV	ROVOR
<i>(All six splittings perform identically)</i>						
form is time-reversal symmetric	yes	yes	yes	yes	yes	yes
splits heat, work, and shadow work	yes	yes	yes	yes	yes	yes
easily incorporates constraints	yes	yes	yes	yes	yes	yes
force evaluations per time step	one	one	one	one	one	one
zero-force MSV	exact	exact	exact	exact	exact	exact
zero-force VAC	exact	exact	exact	exact	exact	exact
zero-force MSD	exact	exact	exact	exact	exact	exact
linear-force virial	$O(\Delta t^2)$	$O(\Delta t^2)$	$O(\Delta t^2)$	$O(\Delta t^2)$	$O(\Delta t^2)$	$O(\Delta t^2)$
<i>(Splittings differ in performance)</i>						
uniform-force terminal drift	exact	exact	exact	exact	$O(\Delta t^2)$	$O(\Delta t^2)$
linear-force MSD	$O(\Delta t^2)$ at n exact at $n + \frac{1}{2}$	$O(\Delta t^2)$ at n exact at $n + \frac{1}{2}$	exact at n	exact at n	$O(\Delta t^2)$	$O(\Delta t^2)$
linear-force MSV	exact at n	exact at n	$O(\Delta t^2)$ at n exact at $n + \frac{1}{2}$	$O(\Delta t^2)$ at n exact at $n + \frac{1}{2}$	$O(\Delta t^4)$ at n	$O(\Delta t^2)$ at n $O(\Delta t^4)$ at $n + \frac{1}{2}$
irreducible Markov chain path action	yes simple	yes requires values at $n + \frac{1}{2}$	no may be ∞	no may be ∞	yes simple	no may be ∞
Hamiltonian dependence for large $\gamma\Delta t$	yes	yes	yes	yes	no	no
can halve number of random variates	yes	yes	yes	yes	no	no
generalizes several popular integrators	yes	no	no	no	no	no

Table 2: Comparison of properties for different splittings. Desiderata are grouped into those satisfied by all six splittings and those where the splittings differ in their performance.

OVRO reduces to the following scheme

$$v(n + \frac{1}{2}) = a v(n - \frac{1}{2}) + \sqrt{\frac{1-a^2}{\beta m}} \mathcal{N}(n) \quad (26a)$$

$$r(n+1) = r(n) + b\Delta t v(n + \frac{1}{2}) . \quad (26b)$$

Ensemble averaging after multiplying Eq. (26a) in turn by $r(n), r(n+1), v(n + \frac{1}{2})$ produces

$$\langle r(n)v(n + \frac{1}{2}) \rangle = a \langle r(n)v(n - \frac{1}{2}) \rangle \quad (27a)$$

$$\langle v^2(n + \frac{1}{2}) \rangle = a \langle v(n - \frac{1}{2})v(n + \frac{1}{2}) \rangle + \frac{1-a^2}{\beta m} \quad (27b)$$

$$\langle v(n - \frac{1}{2})v(n + \frac{1}{2}) \rangle = a \langle v^2(n - \frac{1}{2}) \rangle . \quad (27c)$$

Angled brackets denote an ensemble average. Combining Eq. (27b) and Eq. (27c) and rearranging gives:

$$\langle v^2(n + \frac{1}{2}) \rangle - \frac{1}{\beta m} = a^2 \left(\langle v^2(n - \frac{1}{2}) \rangle - \frac{1}{\beta m} \right) . \quad (28)$$

So for $a < 1$ the MSV will asymptotically approach the Maxwell-Boltzmann result $(\beta m)^{-1}$ regardless of its initial value.

Zero-force velocity autocorrelation function

Requiring the continuous-limit zero-force velocity autocorrelation function fixes the parameter a . For discrete Langevin dynamics, averaging after multiplying Eq. (26a) by $v(n + \frac{1}{2} - \ell)$ for $\ell > 0$ produces

$$\langle v(n + \frac{1}{2} - \ell)v(n + \frac{1}{2}) \rangle = a \langle v(n + \frac{1}{2} - \ell)v(n - \frac{1}{2}) \rangle . \quad (29)$$

Induction using this and the equilibrium result $\langle v^2(n - \frac{1}{2}) \rangle = (\beta m)^{-1}$ reveals that

$$\langle v(n - \frac{1}{2})v(n - \frac{1}{2} + \ell) \rangle = \frac{a^\ell}{\beta m} . \quad (30)$$

Comparison with the zero-force velocity autocorrelation function for continuous-time Langevin dynamics⁴²

$$\langle v(0)v(t) \rangle = \frac{e^{-\gamma t}}{\beta m} , \quad (31)$$

fixes $a = e^{-\gamma \Delta t}$.

Zero-force diffusion coefficient

Requiring the continuous-limit zero-force MSD fixes the time step rescaling b in Eqs. (7c) and (7e). En-

semble averaging after multiplying Eq. (26b) in turn by $r(n), v(n + \frac{1}{2}), v(n - \frac{1}{2})$ produces

$$\langle r(n)r(n+1) \rangle = \langle r^2(n) \rangle + b\Delta t \langle r(n)v(n + \frac{1}{2}) \rangle \quad (32a)$$

$$\langle r^2(n+1) \rangle = \langle r(n)r(n+1) \rangle \quad (32b)$$

$$\begin{aligned} & + b\Delta t \langle r(n+1)v(n + \frac{1}{2}) \rangle \\ \langle r(n+1)v(n + \frac{1}{2}) \rangle & = \langle r(n)v(n + \frac{1}{2}) \rangle \quad (32c) \\ & + b\Delta t \langle v^2(n + \frac{1}{2}) \rangle . \end{aligned}$$

Assuming that the MSV starts (and therefore remains) at

$$\langle v^2(n + \frac{1}{2}) \rangle = \frac{1}{\beta m} , \quad \forall n , \quad (33)$$

and that the particle begins at $r(0) = 0$, combining Eq. (32c), Eq. (27a), and Eq. (33) produces

$$\langle r(n+1)v(n + \frac{1}{2}) \rangle = \frac{b\Delta t}{\beta m} \sum_{i=0}^n a^i = \frac{b\Delta t}{\beta m} \frac{1-a^{n+1}}{1-a} \quad (34a)$$

$$\langle r(n)v(n + \frac{1}{2}) \rangle = \frac{b\Delta t}{\beta m} \frac{a-a^{n+1}}{1-a} . \quad (34b)$$

Combining these results with Eq. (32a) and Eq. (32b) gives

$$\langle r^2(n+1) \rangle = \langle r^2(n) \rangle + \frac{(b\Delta t)^2}{\beta m} \left[2 \frac{1-a^{n+1}}{1-a} - 1 \right] \quad (35a)$$

$$= \frac{(b\Delta t)^2}{\beta m} \left[(n+1) \frac{1+a}{1-a} - \frac{2a(1-a^{n+1})}{(1-a)^2} \right] \quad (35b)$$

$$\approx \frac{(b\Delta t)^2}{\beta m} (n+1) \frac{1+a}{1-a} , \quad n \gg 1 . \quad (35c)$$

Equating this expression to the (Fickian) MSD in the continuous limit $2Dt = 2t/(\beta m \gamma)$ of a particle freely diffusing in one dimension during a total simulation time $t = (n+1)\Delta t$, leads to the effective time step rescaling of Eq. (15),

$$b_{\text{Diff}} = \sqrt{\frac{2}{\gamma \Delta t} \tanh\left(\frac{\gamma \Delta t}{2}\right)} . \quad (36)$$

Terminal drift under uniform external force

Requiring the continuous-limit terminal drift under a uniform external force fixes b in Eqs. (7b) and (7f). The terminal drift equals $\langle r(n+1) - r(n) \rangle / \Delta t = b \langle v(n + \frac{1}{2}\Delta t) \rangle$ once transients have died out and this value stops changing. The velocity reaches its terminal value when

it (on average) doesn't change over a full step of the integrator, satisfied when

$$\langle v(n - \frac{1}{2}) \rangle = \langle v(n + \frac{1}{2}) \rangle = a \langle v(n - \frac{1}{2}) \rangle + (1+a) \frac{b\Delta t}{2} \frac{f}{m}. \quad (37)$$

Thus the terminal drift is

$$b v_{\text{term}} = \frac{b^2 \Delta t}{2} \frac{f}{m} \coth\left(\frac{\gamma \Delta t}{2}\right). \quad (38)$$

The value of b that equates this to the value for the continuous equations of motion, $f/(m\gamma)$, is

$$b_{\text{Drift}}^2 = \frac{2}{\gamma \Delta t} \tanh\left(\frac{\gamma \Delta t}{2}\right) = b_{\text{Diff}}^2. \quad (39)$$

Thus the time rescaling b_{Diff} restoring the continuous-limit zero-force diffusion constant matches the time rescaling b_{Drift} restoring the continuous-limit terminal drift under a uniform external force, and thus applying a single time rescaling $b = b_{\text{Diff}} = b_{\text{Drift}}$ maintains the fluctuation-dissipation relation.

The ORVRO, RVOVR, and VRORV integrators also recover the continuous-limit terminal drift $f/(m\gamma)$ for the same b_{Drift} , Eq. (39). VOROV and ROVOR integrators produce a terminal drift that differs from the continuous-limit value by a factor of $\text{sech}(\gamma \Delta t/2)$. In particular, in the limit of large Δt the terminal drift goes to zero, and the dynamics are thus insensitive to force.

Mean-squared displacement, mean-squared velocity, and virial for linear force

For a time-independent harmonic potential $U = \frac{1}{2}kr^2$, the ORVRO integrator reduces to

$$v(n + \frac{1}{4}) = \sqrt{a} v(n) + \sqrt{\frac{1-a}{\beta m}} \mathcal{N}^+(n) \quad (40a)$$

$$v(n + \frac{1}{2}) = v(n + \frac{1}{4}) - \frac{kb\Delta t}{2m} r(n) \quad (40b)$$

$$r(n + \frac{1}{2}) = r(n) + \frac{b\Delta t}{2} v(n + \frac{1}{2}) \quad (40c)$$

$$r(n + 1) = r(n + \frac{1}{2}) + \frac{b\Delta t}{2} v(n + \frac{1}{2}) \quad (40d)$$

$$v(n + \frac{3}{4}) = v(n + \frac{1}{2}) - \frac{kb\Delta t}{2m} r(n + 1) \quad (40e)$$

$$v(n + 1) = \sqrt{a} v(n + \frac{3}{4}) + \sqrt{\frac{1-a}{\beta m}} \mathcal{N}^-(n + 1). \quad (40f)$$

Ensemble averaging after multiplying Eq. (40a) in turn by $v(n + \frac{1}{4})$, $v(n)$, $r(n)$ produces

$$\langle v^2(n + \frac{1}{4}) \rangle = \sqrt{a} \langle v(n) v(n + \frac{1}{4}) \rangle + \frac{1-a}{\beta m} \quad (41a)$$

$$\langle v(n) v(n + \frac{1}{4}) \rangle = \sqrt{a} \langle v^2(n) \rangle \quad (41b)$$

$$\langle r(n) v(n + \frac{1}{4}) \rangle = \sqrt{a} \langle r(n) v(n) \rangle \quad (41c)$$

This and similar ensemble averages of Eq. (40b) and Eq. (40f) produces a system of 18 linear equations for 18 unknowns. Solving for the MSD and MSV, we find that:

$$\langle r(n + \frac{1}{2})^2 \rangle = \frac{1}{\beta k} \quad (42a)$$

$$\langle r(n)^2 \rangle = \frac{1}{\beta k} \frac{1}{1 - \frac{1}{4} \frac{k}{m} (b\Delta t)^2} \quad (42b)$$

$$\langle v(n)^2 \rangle = \langle v(n + \frac{1}{4})^2 \rangle = \langle v(n + \frac{3}{4})^2 \rangle = \frac{1}{\beta m} \quad (42c)$$

$$\langle v(n + \frac{1}{2})^2 \rangle = \frac{1}{\beta m} \frac{1}{1 - \frac{1}{4} \frac{k}{m} (b\Delta t)^2} \quad (42d)$$

So the MSD at half-steps and the MSV at whole-steps match those of the continuous equations of motion. A similar calculation reveals that ORVRO also produces continuous-limit MSD at half-steps and MSV at whole-steps. Conversely, RVOVR and VRORV produce continuous-limit MSD at whole-steps and MSV at half-steps. Researchers have long known of this friction-independent, frequency-dependent rescaling (as compared to the continuous equations of motion) of the position and velocity fluctuations in similar discrete-time integrators,⁹ but our proposed remedy of a time step rescaling is (to our knowledge) novel. While this time step rescaling would in principle permit the use of larger integration time steps, in more realistic systems numerical stability may impose sufficiently stringent constraints to preclude a substantially larger time step.

Since for each of these four integrators the MSD and MSV attain their continuous-limit values at different points, the virial at any given point in time always differs from the continuous-limit value for each of these four splittings, with $O(\Delta t^2)$ error. VOROV and ROVOR integrators produce MSD with $O(\Delta t^2)$ error, and MSV with $O(\Delta t^4)$ error at timepoints n and $n + \frac{1}{2}$, respectively, and thus virials with at least $O(\Delta t^2)$ error.

Multiple dimensions

This family of integrators is trivially extended to multiple degrees of freedom. The position r , velocity v , and force f become vectors \mathbf{r} , \mathbf{v} , and \mathbf{f} , respectively. The mass m becomes a diagonal matrix \mathbf{m} . The normal variates $\mathcal{N}^\pm(n)$ become random vectors $\mathbf{N}^\pm(n)$, with averages and covariance

$$\langle \mathbf{N}_i^\rho(n) \rangle = \mathbf{0}, \quad \langle \mathcal{N}_i^\rho(m) \mathcal{N}_j^\sigma(n) \rangle = \delta_{ij} \delta_{mn} \delta_{\rho\sigma}, \quad (43)$$

where $\rho, \sigma \in \{+, -\}$. The mass m and coefficients a and b become diagonal matrices \mathbf{m} , \mathbf{a} , and \mathbf{b} , respectively, such that $a_{ij} = \delta_{ij} \exp(-\gamma_i \Delta t)$ and

$$b_{ij} = \delta_{ij} \sqrt{\frac{2}{\gamma_i \Delta t} \tanh\left(\frac{\gamma_i \Delta t}{2}\right)}. \quad (44)$$

The resulting equations for OVRVO are:

$$\mathbf{v}(n + \tfrac{1}{4}) = \mathbf{a}^{1/2} \cdot \mathbf{v}(n) + \left(\frac{1}{\beta} (\mathbf{I} - \mathbf{a}) \cdot \mathbf{m}^{-1} \right)^{1/2} \cdot \mathbf{N}^+(n) \quad (45a)$$

$$\mathbf{v}(n + \tfrac{1}{2}) = \mathbf{v}(n + \tfrac{1}{4}) + \frac{\Delta t}{2} \mathbf{b} \cdot \mathbf{m}^{-1} \cdot \mathbf{f}(n) \quad (45b)$$

$$\mathbf{r}(n + \tfrac{1}{2}) = \mathbf{r}(n) + \frac{\Delta t}{2} \mathbf{b} \cdot \mathbf{v}(n + \tfrac{1}{2}) \quad (45c)$$

$$\mathcal{H}(n) \rightarrow \mathcal{H}(n + 1) \quad (45d)$$

$$\mathbf{r}(n + 1) = \mathbf{r}(n + \tfrac{1}{2}) + \frac{\Delta t}{2} \mathbf{b} \cdot \mathbf{v}(n + \tfrac{1}{2}) \quad (45e)$$

$$\mathbf{v}(n + \tfrac{3}{4}) = \mathbf{v}(n + \tfrac{1}{2}) + \frac{\Delta t}{2} \mathbf{b} \cdot \mathbf{m}^{-1} \cdot \mathbf{f}(n + 1) \quad (45f)$$

$$\mathbf{v}(n + 1) = \mathbf{a}^{1/2} \cdot \mathbf{v}(n + \tfrac{3}{4}) + \left(\frac{1}{\beta} (\mathbf{I} - \mathbf{a}) \cdot \mathbf{m}^{-1} \right)^{1/2} \cdot \mathbf{N}^-(n + 1), \quad (45g)$$

for identity matrix \mathbf{I} .

Metropolization and time step scaling

The shadow work (resulting from the finite time step of discrete Langevin integrators) drives the system out of equilibrium.⁷ Metropolization⁴³ is a popular method to recover the equilibrium distribution (though at the cost of unphysical dynamics). For example, in generalized hybrid Monte Carlo,^{13,44} the shadow work is used in a Metropolis acceptance step, which can improve integrator stability.⁴⁵ In order to maintain a reasonable acceptance rate the time step Δt must scale with the

dimension d as $d^{-1/4}$, if the different degrees of freedom are uncorrelated.⁴⁶ By similar arguments, when omitting the Metropolis step, achieving statistically robust work-reweighted expectations (or minimizing departures from the desired distribution by keeping the shadow work small in magnitude) also requires scaling the time step Δt as $d^{-1/4}$. As a result, the number of time steps (and hence force evaluations) required to simulate a given time interval to a given accuracy scales as $d^{1/4}$.

Notes and References

- (1) Swope, W. C.; Andersen, H. C.; Berens, P. H.; Wilson, K. R. A Computer Simulation Method for the Calculation of Equilibrium Constants for the Formation of Physical Clusters of Molecules: Application to Small Water Clusters. *J. Chem. Phys.* **1982**, *76*, 637–649.
- (2) Allen, M. P.; Tildesley, D. J. *Computer Simulation of Liquids*; Oxford University Press: Oxford, 1989.
- (3) Frenkel, D.; Smit, B. *Understanding Molecular Simulation*, 2nd ed.; Academic Press: San Diego, 2002.
- (4) Leach, A. *Molecular Modeling: Principles and Applications*, 2nd ed.; Prentice Hall: Harlow, England, 2001.
- (5) Schlick, T. *Molecular Modeling and Simulation*, 3rd ed.; Springer: New York, 2010.
- (6) Jarzynski, C. Equalities and Inequalities: Irreversibility and the Second Law of Thermodynamics at the Nanoscale. *Annu. Rev. Condens. Matter Phys.* **2011**, *2*, 329–351.
- (7) Sivak, D. A.; Chodera, J. D.; Crooks, G. E. Using Nonequilibrium Fluctuation Theorems to Understand and Correct Errors in Equilibrium and Nonequilibrium Simulations of Discrete Langevin Dynamics. *Phys. Rev. X* **2013**, *3*, 011007.
- (8) Langevin, P. Sur la Théorie du Mouvement Brownien. *C. R. Acad. Sci. (Paris)* **1908**, *146*, 530–533, English Translation: *Am. J. Phys.* **65**, 1079–1081 (1997).

- (9) Pastor, R. W.; Brooks, B. R.; Szabo, A. An Analysis of the Accuracy of Langevin and Molecular Dynamics Algorithms. *Mol. Phys.* **1988**, *65*, 1409–1419.
- (10) Stoltz, G. Path Sampling with Stochastic Dynamics: Some New Algorithms. *J. Comput. Phys.* **2007**, *225*, 491–508.
- (11) Minh, D. D. L.; Chodera, J. D. Optimal Estimators and Asymptotic Variances for Nonequilibrium Path-Ensemble Averages. *J. Chem. Phys.* **2009**, *131*, 134110.
- (12) Chodera, J. D.; Swope, W. C.; Noé, F.; Prinz, J.-H.; Shirts, M. R.; Pande, V. S. Dynamical Reweighting: Improved Estimates of Dynamical Properties from Simulations at Multiple Temperatures. *J. Chem. Phys.* **2011**, *134*, 244107.
- (13) Lelièvre, T.; Rousset, M.; Stoltz, G. *Free Energy Computations: A Mathematical Perspective*; Imperial College Press: London, 2010.
- (14) The *shadow work* denotes the net energy change during deterministic symplectic substeps that, due to their discretization, do not preserve the system Hamiltonian. For a detailed discussion of shadow work and its importance in nonequilibrium fluctuation relations, see Ref. 7.
- (15) Brünger, A.; Brooks III, C. L.; Karplus, M. Stochastic Boundary Conditions for Molecular Dynamics Simulations of ST2 Water. *Chem. Phys. Lett.* **1984**, *105*, 495–500.
- (16) Athènes, M. A Path-Sampling Scheme for Computing Thermodynamic Properties of a Many-Body System in a Generalized Ensemble. *Eur. Phys. J. B* **2004**, *38*, 651–663.
- (17) Adjanor, G.; Athènes, M. Gibbs Free-Energy Estimates From Direct Path-Sampling Computations. *J. Chem. Phys.* **2005**, *123*, 234104.
- (18) Adjanor, G.; Athènes, M.; Calvo, F. Free Energy Landscape From Path-Sampling: Application to the Structural Transition in LJ₃₈. *Eur. Phys. J. B* **2006**, *53*, 47–60.
- (19) Vanden-Eijnden, E.; Ciccotti, G. Second-Order Integrators for Langevin Equations With Holonomic Constraints. *Chem. Phys. Lett.* **2006**, *429*, 310–316.
- (20) Bussi, G.; Parrinello, M. Accurate Sampling Using Langevin Dynamics. *Phys. Rev. E* **2007**, *75*, 056707.
- (21) Bussi, G.; Zykova-Timan, T.; Parrinello, M. Isothermal-Isobaric Molecular Dynamics Using Stochastic Velocity Rescaling. *J. Chem. Phys.* **2009**, *130*, 074101.
- (22) Izaguirre, J. A.; Sweet, C. R.; Pande, V. S. Multiscale Dynamics of Macromolecules Using Normal Mode Langevin. *Pac. Symp. Biocomput.* **2010**, 240–251.
- (23) Bou-Rabee, N.; Owhadi, H. Long-Run Behavior of Variational Integrators in the Stochastic Context. *SIAM J. Numer. Anal.* **2010**, *48*, 278–297.
- (24) Lelièvre, T.; Rousset, M.; Stoltz, G. Langevin Dynamics With Constraints and Computation of Free Energy Differences. *Math. Comput.* **2012**, *81*, 2071–2125.
- (25) Leimkuhler, B.; Matthews, C. Rational Construction of Stochastic Numerical Methods for Molecular Sampling. *Appl. Math. Res. Express* **2013**, *2013*, 34–56.
- (26) Zwanzig, R. *Nonequilibrium Statistical Mechanics*; Oxford University Press: New York, 2001.
- (27) Risken, H. *The Fokker-Planck Equation: Methods of Solution and Applications*, 3rd ed.; Springer-Verlag: Berlin, 1996.
- (28) Tuckerman, M. E.; Berne, B. J.; Martyna, G. J. Reversible Multiple Time Scale Molecular Dynamics. *J. Chem. Phys.* **1992**, *97*, 1990–2001.
- (29) Sexton, J. C.; Weingarten, D. H. Hamiltonian Evolution for the Hybrid Monte Carlo Algorithm. *Nucl. Phys. B* **1992**, *380*, 665–677.
- (30) Trotter, H. F. On the Product of Semi-Groups of Operators. *Proc. Amer. Math. Soc.* **1959**, *10*, 545–551.
- (31) Note that, even for a time-independent Hamiltonian, the sampled distribution will differ from the true canonical measure $\mu(r, v) \propto \exp[-\mathcal{H}(r, v)]$ in a time step-dependent manner⁷.
- (32) Uhlenbeck, G. E.; Ornstein, L. S. On the Theory of the Brownian Motion. *Phys. Rev.* **1930**, *36*, 823–841.

- (33) Yang, S.; Witkoskie, J. B.; Cao, J. Single-Molecule Dynamics of Semiflexible Gaussian Chains. *J. Chem. Phys.* **2002**, *117*, 11010–11023.
- (34) Ermak, D. L.; Yeh, Y. Equilibrium Electrostatic Effects on the Behavior of Polyions in Solution: Polyion-Mobile Ion Interaction. *Chem. Phys. Lett.* **1974**, *24*, 243–248.
- (35) Maruyama, G. Continuous Markov Processes and Stochastic Equations. *Rend. Circ. Matem. Palermo* **1955**, *4*, 48–90.
- (36) Andersen, H. C. Rattle: A “Velocity” Version of the Shake Algorithm for Molecular Dynamics Calculations. *J. Comp. Phys.* **1983**, *52*, 24–34.
- (37) Leimkuhler, B. J.; Skeel, R. D. Symplectic Numerical Integrators in Constrained Hamiltonian Systems. *J. Comp. Phys.* **1994**, *112*, 117–125.
- (38) Dellago, C.; Bolhuis, P.; Csajka, F. S.; Chandler, D. Transition Path Sampling and the Calculation of Rate Constants. *J. Chem. Phys.* **1998**, *108*, 1964–1977.
- (39) Dellago, C.; Bolhuis, P. G.; Geissler, P. L. Transition Path Sampling. *Adv. Chem. Phys.* **2002**, *123*, 1–78.
- (40) Athènes, M.; Adjanor, G. Measurement of Nonequilibrium Entropy From Space-Time Thermodynamic Integration. *J. Chem. Phys.* **2008**, *129*, 024116.
- (41) Schlick, T.; Barth, E.; Mandziuk, M. Biomolecular Dynamics at Long Timesteps: Bridging the Timescale Gap Between Simulation and Experimentation. *Annu. Rev. Biophys. Biom.* **1997**, *26*, 181–222.
- (42) Chandler, D. *Introduction to Modern Statistical Mechanics*; Oxford University Press: Oxford, 1987.
- (43) Duane, S.; Kennedy, A. D.; Pendleton, B. J.; Roweth, D. Hybrid Monte-Carlo. *Phys. Lett. B* **1987**, *195*, 216–222.
- (44) Horowitz, A. M. A Generalized Guided Monte Carlo Algorithm. *Phys. Lett. B* **1991**, *268*, 247–252.
- (45) Bou-Rabee, N.; Vanden-Eijnden, E. A Patch That Imparts Unconditional Stability to Explicit Integrators for Langevin-Like Equations. *J. Comput. Phys.* **2012**, *231*, 2565–2580.
- (46) Beskos, A.; Pillai, N. S.; Roberts, G. O.; Sanz-Serna, J. M.; Stuart, A. M. Optimal Tuning of the Hybrid Monte-Carlo Algorithm. *arXiv* **2010**, 1001.4460.